^{119}Sn Mössbauer spectroscopy of Sn–O nanoparticles prepared by levitation-jet aerosol synthesis

Maxim V. Kuznetsov,*[a] Denis A. Pankratov,[b] Iurii G. Morozov,[c] Ivan P. Parkin,[d] Alexey V. Safonov[a] and Olga V. Belousova[c]

[a] *All-Russian Research Institute for Civil Defense and Emergencies, EMERCOM of Russia, 121352 Moscow, Russian Federation. E-mail: maxim1968@mail.ru*
[b] *Department of Chemistry, M. V. Lomonosov Moscow State University, 119991 Moscow, Russian Federation*
[c] *A. G. Merzhanov Institute of Structural Macrokinetics and Materials Science, Russian Academy of Sciences, 142432 Chernogolovka, Moscow Region, Russian Federation*
[d] *Department of Chemistry, Materials Chemistry Research Centre, University College London, WC1H 0AJ London, United Kingdom*

Sn–O nanoparticles were prepared by levitation-jet aerosol synthesis and found to exhibit ferromagnetic behavior. X-ray powder diffraction analysis and ^{119}Sn Mössbauer spectroscopy confirmed these nanoparticles consist of β-Sn, SnO and SnO_2 phases. The maximum specific magnetization was observed for nanoparticles containing the SnO/SnO_2 interface.

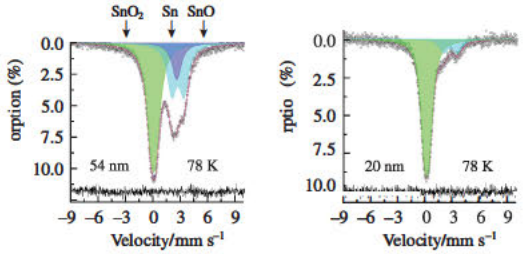

Keywords: levitation jet generator, nanoparticles, tin monoxide, tin dioxide, Mössbauer spectra, room-temperature ferromagnetism, X-ray diffraction.

Tin dioxide (SnO_2) is an n-type semiconductor with a wide bandgap and a pronounced potential in spintronic applications.[1] Undoped SnO_2 nanoparticles (NPs) were studied by various methods, including magnetic measurements, which revealed a low value of the maximum saturation magnetization at room temperature and convincingly indicated that room-temperature ferromagnetism is an intrinsic feature of NPs related to structural defects.[2] This work used a levitation-jet generator[3] to prepare Sn–O NPs[4] and applied ^{119}Sn Mössbauer spectroscopy to deepen such investigations.†

Transmission electron microscopy (TEM) images of Sn–O NPs[4] show small spherical nanoparticles (Figure 1). Table 1 contains essential characteristics† of Sn–O NPs such as mean particle size (d) and specific surface area (S) as well as synthesis conditions: constant He flow rate (500 dm^3 h^{-1}), airflow rate, Sn feed rate and total gas pressure (P). All NPs were ferromagnetic with a saturation magnetization (σ_s)† equal to several memu g^{-1} (see Table 1).

Analysis of XRD patterns† revealed only reflections from β-Sn (JCPDS card no. 86-2265), SnO (JCPDS card no. 78-1913) and SnO_2 (JCPDS card no. 71-0652).[5] We assessed percentages of observed phases using the Rietveld method for full profile analysis of XRD patterns (Table 2).

In the region of low velocities of the Mössbauer spectra of the samples, resonance absorption of a complex shape was observed, which indicates that the experimental spectrum is a sum of partial subspectra. At the same time, the shape and intensity of the spectra are susceptible to temperature changes (Figure 2). Obviously, with a temperature change, the partial subspectra change their intensity independently of each other, which is the reason for the change in the shape of the entire spectrum. The spectra were

Table 1 The characteristics of Sn O NPs and the conditions for their synthesis.

Sample	d/nm	S/m^2 g^{-1}	σ_s/memu g^{-1}	Synthesis conditions: Sn feed rate/ g h^{-1}	Airflow rate/dm^3 h^{-1}	P/Torr
T1	54(1)	15.2(1)	1.40(2)	15	95	75
T2	50(1)	20.2(1)	0.60(2)	25	430	300
T3	38(1)	38.7(1)	6.10(2)	20	430	75
T4	20(1)	45.9(1)	6.50(2)	20	180	50
T5	13(1)	47.5(1)	4.00(2)	20	120	50

The specific surface area of NPs was studied using four point measurements of nitrogen physical sorption by the BET method on a Sorbi® M device (OOO META).

Magnetic measurements at 300 K were carried out on a Quantum Design SQUID vibrating sample magnetometer.

The crystal structure and phase composition of NPs were determined by powder X ray diffraction (XRD) on a Siemens D5000 diffractometer using CuKα radiation.

† The ^{119}Sn Mössbauer absorption spectra were obtained on an MS 1104Em express Mössbauer spectrometer (ZAO Kordon). The γ radiation source was ^{119m}Sn in a $CaSnO_3$ matrix with an activity of 2.5 mCi (Ritverc JSC). The spectra were recorded both at room temperature without temperature control (296 ± 3 K) and at the liquid nitrogen temperature with temperature control (77.5 ± 0.5 K). All spectra were recorded with a noise/signal ratio of 2%. A model description of the experimental data was performed for high resolution Mössbauer spectra (1024 points) using the SpectrRelax 2.8 software. For this, the spectra were described by combinations of singlet and symmetric doublet resonance lines with a fixed intensity/width ratio. Isomer shifts (δ) are reported relative to $BaSnO_3$.

The morphology and size of NPs were examined using a JEOL JEM 1200EX II transmission electron microscope.

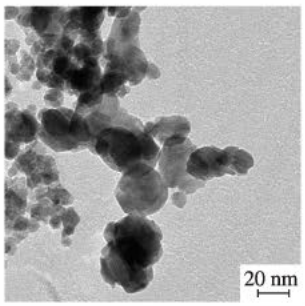

Figure 1 TEM image of sample T4.

described by a set of three subspectra of SnO_2, SnO and β-Sn (see Figure 2 and Table 2). The parameters of the first subspectrum were reliably determined and were relatively stable in all the samples. The other two subspectra are distinguished by similar values of isomeric shifts, which, due to the large width of the resonance lines, the small particle size and the high defectiveness of the structures, made it difficult to determine them reliably. In these cases, the parameters of the minor subspectra were fixed based on the data for sample T5, where the SnO parameters can be determined relatively reliably. The obtained Mössbauer parameters with the assumption of a temperature shift agree with the literature data.[6] In the Mössbauer spectra of samples T2, T4 and T5 at room temperature, among other parameters, extended absorptions described by a very wide singlet were observed. They can be associated with the intermediate oxide (IO),[7] the presence of NPs or both (taking into account the strong temperature dependence of the magnitude of this effect).

It is known that, due to the low Debye temperature, metallic β-tin exhibits a strong temperature dependence of the recoil-free fraction *f* in the Mössbauer effect (0.75, 0.446 and 0.039 at 4.2, 80 and 300 K, respectively).[8,9] Moreover, for tin nanoparticles, an even more significant decrease in the *f* value can be observed.[10–12] The recoil-free fraction *f* for SnO does not change so much with temperature (from 0.3 at 295 K to 0.8 at 4.2 K),[9] but it is significant enough not to take it into account when determining the relative content of the components. For crystalline SnO_2, the temperature dependence of the recoil-free fraction *f* is not very large (from 0.56 at 295 K to 0.77 at 4.2 K). However, for the amorphous and hydrated forms, it increases again.[9] For the samples under discussion,

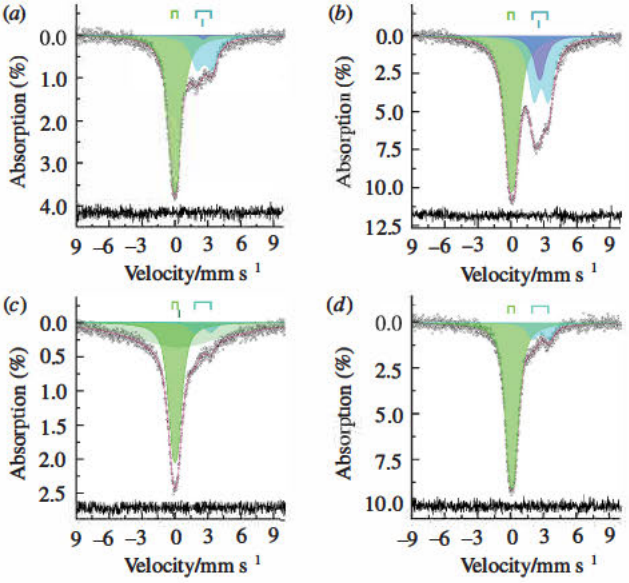

Figure 2 ^{119}Sn Mössbauer spectra of samples (*a*),(*b*) T1 and (*c*),(*d*) T4 at (*a*),(*c*) 296 and (*b*),(*d*) 78 K and their model description.

even for the SnO_2 subspectrum, the temperature dependence of the intensity of the resonance lines turned out to be noticeably stronger than could be expected based on the literature data for the recoil-free fraction *f*. This discrepancy may indicate a decrease in the recoil-free fraction *f* for nanosized particles of material, including SnO_2. All this is the reason for the strong temperature dependence of the intensity of the corresponding subspectra. Hence, the most reliable data on the relative content of components in the samples under study are the data of low-temperature measurements. Therefore, even though the relative areas of the subspectra are significantly dependent on temperature, the relative areas of the subspectra determined at low temperatures are in good agreement with the XRD data (see Table 2).

Comparison of the data in Tables 1 and 2 shows that the maximum specific magnetization occurred when the phase composition of NPs was SnO/SnO_2. This result suggested that the region of interface between these phases is the main region of ferromagnetic ordering.[4]

In summary, it was demonstrated that ferromagnetic Sn–O nanoparticles prepared by the levitation-jet aerosol synthesis

Table 2 The parameters of model descriptions of ^{119}Sn Mössbauer spectra compared to XRD data of synthesized Sn–O NPs.

Sample	Subspectrum no.	^{119}Sn Mössbauer spectral parameters[a]								XRD data	
		T = 296 K				*T* = 78 K				Content (%)	Phase
		δ/mm s^{-1}	Δ/mm s^{-1}	Γ_{exp}/mm s^{-1}	S_{rel} (%)	δ/mm s^{-1}	Δ/mm s^{-1}	Γ_{exp}/mm s^{-1}	S_{rel} (%)		
T1	1	0.01(1)	0.47(2)	1.13(3)	72.4(5)	0.05(1)	0.53(1)	1.18(2)	53.1(3)	48.4	SnO_2
	2	2.66(1)	1.33(5)	1.29(5)	27(1)	2.71(1)	1.32(2)	1.24(3)	33.7(8)	38.3	SnO
	3	2.56(1)		0.6(6)	1(1)	2.58(1)		1.24(3)	13.2(7)	13.3	β Sn
T2	1	0.00(1)	0.50(1)	1.01(3)	61(4)	0.05(1)	0.52(2)	1.24(3)	100.0	100.0	SnO_2
	4	0.2(1)		10(2)	39(4)						IO‖NP
T3	1	0.01(1)	0.48(1)	1.02(3)	89.3(5)	0.06(1)	0.55(1)	1.09(2)	81.6(5)	74.7	SnO_2
	2	2.66(3)	1.43(5)	1.04(8)	10.7(5)	2.69(2)	1.54(3)	1.19(5)	18.4(5)	25.3	SnO
T4	1	0.01(1)	0.47(2)	1.13(4)	41.1(7)	0.06(1)	0.54(1)	1.05(2)	86.1(5)	79.4	SnO_2
	2	2.53(3)	1.50(5)	0.9(1)	3.8(5)	2.70(2)	1.48(4)	1.15(6)	13.9(5)	20.6	SnO
	4	0.41(7)		9.5(3)	55(1)						IO‖NP
T5	1	0.01(1)	0.50(1)	1.00(3)	67(4)	0.05(1)	0.58(1)	1.22(3)	79.8(5)	72.9	SnO_2
	2	2.63(3)	1.38(5)	1.3(1)	14(2)	2.73(1)	1.44(4)	1.06(5)	17.4(9)	24.3	SnO
	3					2.71(5)		1.06(5)	2.8(7)	2.8	β Sn
	4	0.0(3)		5.2(8)	20(6)						IO‖NP

[a] Here, δ is the isomer shift, Δ is the quadrupole splitting, Γ_{exp} is the linewidth, and S_{rel} is the relative area of the corresponding subspectrum.

exhibit Mössbauer spectra with three main components: β-Sn, SnO and SnO_2 and have the maximum specific magnetization for nanoparticles containing the SnO/SnO_2 interface. We assume that certain localized states present at this interface, such as interacting oxygen vacancies, are responsible for the observed magnetic behavior of the nanoparticles under study.[13]

References

1 P. Venkateswara Reddy, S. Venkatramana Reddy and B. Sreenivasulu, *J. Mater. Sci.: Mater. Electron.*, 2021, **32**, 8195.
2 M. Dinesh, R. Ravindran, V. Rukkumani, K. Srinivasan and M. Saravanakumar, *Int. J. Nanosci.*, 2020, **19**, 1850045.
3 Yu. G. Morozov, O. V. Belousova, M. V. Kuznetsov, D. Ortega and I. P. Parkin, *J. Mater. Chem.*, 2012, **22**, 11214.
4 M. V. Kuznetcov, O. V. Belousova, D. Ortega and Iu. G. Morozov, *Inorg. Mater.*, 2014, **50**, 793 (*Neorg. Mater.*, 2014, **50**, 856).
5 A. A. Ulyankina, A. B. Kuriganova and N. V. Smirnova, *Mendeleev Commun.*, 2019, **29**, 215.
6 L. Protesescu, A. J. Rossini, D. Kriegner, M. Valla, A. de Kergommeaux, M. Walter, K. V. Kravchyk, M. Nachtegaal, J. Stangl, B. Malaman, P. Reiss, A. Lesage, L. Emsley, C. Copéret and M. V. Kovalenko, *ACS Nano*, 2014, **8**, 2639.
7 F. Gauzzi, B. Verdini, A. Maddalena and G. Principi, *Inorg. Chim. Acta*, 1985, **104**, 1.
8 C. Hohenemser, *Phys. Rev.*, 1965, **139**, A185.
9 P. S. Cook, J. D. Cashion and P. J. Cassidy, *Fuel*, 1985, **64**, 1121.
10 G. E. J. Koops, S. Nauwelaerts, R. Venegas, A. Vantomme and H. Pattyn, *Nucl. Instrum. Methods Phys. Res., Sect. B*, 2001, **178**, 93.
11 R. Mantovan, A. Debernardi and M. Fanciulli, *J. Phys.: Condens. Matter*, 2008, **20**, 385201.
12 G. E. J. Koops, H. Pattyn, A. Vantomme, S. Nauwelaerts and R. Venegas, *Phys. Rev. B*, 2004, **70**, 235410.
13 K. Ackland and J. M. D. Coey, *Phys. Rep.*, 2018, **746**, 1.